Energy Reports 7 (2021) 6876–6886

Contents lists available at ScienceDirect

Energy Reports

journal homepage: www.elsevier.com/locate/egyr

Research paper

Optimal parameters estimation of the PEMFC using a balanced version of Water Strider Algorithm

Rahmad Syah[a,*], Lawal Adedoyin Isola[b,c,d,e], John William Grimaldo Guerrero[f], Wanich Suksatan[g], Denok Sunarsi[h], Marischa Elveny[j], Ayad F. Alkaim[i], Lakshmi Thangavelu[k], Surendar Aravindhan[l]

[a] Faculty of Engineering, Universitas Medan Area, Medan, Indonesia
[b] Department of Accounting and Finance, Landmark University, Omu-Aran, Nigeria
[c] Sustainable Development Goal 17 (Partnership for the Goals) Research Cluster, Landmark University, Nigeria SDG 8 (Decent Work and Economic Growth) Research Cluster, Landmark University, Nigeria
[d] SDG1(Zero Hunger) Research Cluster Landmark University, Nigeria
[e] SDG6(Clean Energy) Research Cluster Landmark University, Nigeria
[f] Department of Energy, Universidad de la Costa, Barranquilla, Colombia
[g] Faculty of Nursing, HRH Princess Chulabhorn College of Medical Science, Chulabhorn Royal Academy, Bangkok, 10210, Thailand
[h] Universitas Pamulang, Tangerang Selatan, Banten, Indonesia
[i] Data Science & Computational Intelligence Research Group, Universitas Sumatera Utara, Medan, Indonesia
[j] College of Science for Women/University of Babylon, Iraq
[k] Department of Pharmacology, Saveetha Dental College and Hospital, Saveetha Institute of Medical and Technical Sciences, Saveetha University, Chennai, India
[l] Department of Pharmacology, Saveetha Dental College and Hospital, Saveetha Institute of Medical and Technical Sciences, Chennai , India,

ARTICLE INFO

Article history:
Received 6 August 2021
Received in revised form 23 September 2021
Accepted 3 October 2021
Available online xxxx

Keywords:
Proton exchange membrane fuel cell
Model parameters estimation
Balanced Water Strider optimizer
A total of squared error
Terminal voltage
Practical test case

ABSTRACT

Recently, much attention was paid to the application of renewable energy in environmental issues. Meanwhile, the fuel cell industry, which is considered an environmentally friendly industry, is one of the important components of this project. They are in fact devices for the direct conversion of chemical energy into electrical energy by an electrochemical reaction without the need for any mechanical parts. In this study, it is attempted to model one of their important types, called proton exchange membrane fuel cells, so that it can be used in predicting the behavior of the fuel cell and examining various parameters affecting the performance of the cell. The main idea is to optimal parameters estimation for the proton exchange membrane fuel cells by minimizing the total Squared Error value between the empirical output voltage and the approximated output voltage. For giving better results in terms of accuracy and reliability, a new design of a metaheuristic called the balanced Water Strider Algorithm is utilized. The results of the suggested method are finally validated by comparison with several latest optimizers applied on a practical test case. After running all of the optimizers 30 times independently, the proposed method with minimum absolute error equals 3.4831e−4 shows the best results toward the others.

1. Introduction

Fuel cells are a new technology for generating energy that produces high-efficiency electricity from a direct combination of fuel and oxidant without causing environmental or noise pollution. Currently, the most popular fuel cell is the hydrogen type, which is produced by the reaction between hydrogen and oxygen, water, heat, and electricity (Ghiasi et al., 2019). Fuel cells consist of three main parts: the cathode, the anode, and the electrolyte. Electrolytes play an important role in the fuel cell and allow ions to pass through the cell with the necessary selectivity. In recent years, the use of polymers as electrolytes in the manufacture of hydrogen fuel cells has become common. These kinds of fuel cells are called Proton exchange membrane fuel cells (PEMFCs) (Mir et al., 2020). Also, the ability to generate power between several watts to several megawatts has made it possible to use them in different utilizations, from propulsion for trains and ships to power production to sensors (Yu et al., 2020). Despite several advantages, in their commercialization, the most significant obstacles are less lifespan and high price.

* Corresponding author.
E-mail address: syahrahmad1985@gmail.com (R. Syah).

https://doi.org/10.1016/j.egyr.2021.10.057
2352-4847/

Proton exchange membrane fuel cells can be replaced by internal combustion engines for transport applications which is because they have outstanding characteristics such as high efficiency, solid electrolyte, production of electrical energy without making pollution, diversity, no noise, and short start-up time. Besides transportation uses, the application of these batteries in portable devices like cell phones, laptops, etc. is also incrementing rapidly, and to become commercial, their price must be reduced and their performance-optimized. The chemical energy of a fuel is converted into electrical energy by these cells, and heat and water are their only output.

Computational modeling of a fuel cell is an analytical typical example of the physical phenomena also the electrochemical procedures that govern the operation of a fuel cell. Computational models of polymer membrane fuel cells are applied for two objectives (Hamian et al., 2018). One way to learn more is the complicated physical phenomena that control fuel cell operation. For example, due to the nature of the fuel cell, it is difficult for some physical phenomena to be achieved in their natural place and this information is defined by an analytical technique (Bagheri et al., 2018; Cai et al., 2019; Hosseini Firouz and Ghadimi, 2016). Computational techniques are as well as applied as a tool for fuel cell design (Ye et al., 2020). As an example, fuel cell modeling can be applied to guide a study of battery design parameters to evaluate battery performance.

Models depending on our goals can be considered simple and focus on one or more physical phenomena, or they can be complex and comprehensive (Fan et al., 2020a). The advantage of the simple model is that the information can be obtained in the shortest possible time. Because a simple computational model can be solved much faster than a comprehensive model (Yu and Ghadimi, 2019; Saeedi et al., 2019; Meng et al., 2020). But instead, comprehensive models give us more information. This model includes a multiplication of equations that describes the processes within the system. Furthermore, formulas that define the materials' electrochemical and physical features used in the cell are needed for modeling (Razmjooy et al., 2017).

After preparing the equations of the mathematical model, the model should be solved (Aghajani and Ghadimi, 2018). Since several model parameters are variable and unknown, a method must be considered to select the appropriate value for them (Liu et al., 2020). Several types of research were performed for proper choice of the unfamiliar variables in PEMFCs. Especially, recently, the application of using optimization-based methods for this purpose is exponentially increasing. For instance, Yuan et al. (2020) introduced an optimum technique to model PEMFCs (Tian et al., 2020). The technique was relied on using the Developed Sunflower Optimizer (DSFO) as a tool for minimizing the error between the observed and the produced voltage outputs of the PEMFCs. To verify the technique, it was applied to two practical models and a comparison of its results with some various methods was carried out (Fei et al., 2019). Simulation achievements displayed the higher effectiveness of the technique toward the compared methods.

Guo et al. (2020b) suggested a new optimized procedure for variable estimation of a 50 kW PEMFC using the economic-functional technique. The major concept was to lessen the overall cost for the stack construction. The cost function used in this study is the total of the fuel cell stack expense and its auxiliaries by assuming air and hydrogen stoichiometric coefficient, the current density, the system temperature, system pressure. To solve the minimization problem, Grass Fibrous Root Optimizer (MGRO) has been used. Simulation achievements indicated that using the suggested technique has a good dominance over some other state-of-the-art methods.

Xu et al. (2020) suggested another method for optimal variables recognition for high-temperature proton exchange membrane fuel cells (HT-PEMFCs). Therefore, the exergy efficiency and the irreversibility of the fuel cell have been evaluated under various conditions and the impact of pressure and temperature were assessed. The parameters of the HT-PEMFC were optimized by Modified Manta-Ray Foraging Optimization Algorithm. Achievements indicated that the suggested algorithm increases the efficiency of the modeling against some other analyzed methods.

Yang et al. (2020) introduced another related work for optimizing the model of PEMFC. The aim was to lessen the total squared error (SSE) magnitude between the empirical produced voltage and the approximated produced voltage. To give an optimal viewpoint, Improved Barnacles Mating Optimizer (IBMO) was utilized. The method was then validated by comparing it with some renowned approaches. Simulation results indicated that using IBMO was given the minimum value of SSE compared with some other similar works which showed its better efficiency toward the others.

Yin and Razmjooy (2020) proposed another optimized method to optimal model recognition of the PEMFCs. The technique was relied on the optimization of the model by giving a combination between of deep-belief network and an Improved Deer Hunting Optimizer. Then the method has been employed for evolving the effectiveness of the parameters in the PEMFC stack. Several conditions were assessed for operation verification of the technique that is performed with a comparison of its achievements with some other methods. Final achievements showed the preeminence of the suggested technique against the others.

As understood from the literature, the applications of the metaheuristic optimizers for optimal selection of the PEMFC models are getting increasing in a high ratio. The main disadvantage for most metaheuristics in this subject is their weakness in avoiding the local minima and achieve global optimal. In this paper, a new optimization methodology has been used with a different modeling equation for improving the performance of the model. The main contributions of the proposed method are given below:

- Design an optimal model for the PEMFCs
- Minimize the total Squared Error between the empirical and the estimated output voltage.
- A new balanced Water Strider Algorithm (bWSA) is used for minimization.
- The results are validated by comparison with several latest optimizers and a practical test case.

2. Modeling

A fuel cell is an energy conversion device in which the chemical energy of the reactants is converted directly into electrical energy during an exothermic process. In general, the reactions that occur in the catalyst layer of the polymer membrane fuel cell include the hydrogen oxidation reaction at the anode and the decline of oxygen at the cathode.

$$\textit{Anode side}: \mathrm{H_2} \rightarrow 2\mathrm{H}^+ + 2\mathrm{e}^- \tag{1a}$$

$$\textit{Cathode side}: 4\mathrm{H}^+ + \mathrm{O_2} + 4\mathrm{e}^- \rightarrow 2\mathrm{H_2O} \tag{1b}$$

And, the main reaction for a PEMFC is as below:

$$\textit{Overall reaction}: \mathrm{H_2} + \mathrm{O_2} \rightarrow 2\mathrm{H_2O} \tag{1c}$$

The concept of this model is shown in Fig. 1.

Based on the fuel cell's polarization curve, three sections are important. The first part relates to the activation polarization that poses powerful non-linearity. This is triggered by the frailty on the active surface of the electrodes of the reactions taking place.

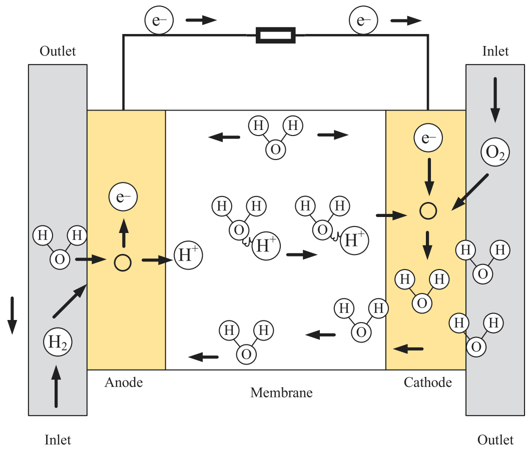

Fig. 1. The model of a polymer membrane fuel cell.

In the next section, ohmic polarization is primarily caused by ohmic losses consisting of membrane resistance and building material electrical resistance and interaction resistance.

Finally, the third part includes the polarization of concentration. As a reactant is used by electrochemical reaction at the electrode, a loss of potential is exist because of the weakness of the surrounding material to sustain the primary reactant concentration; that is, a gradient of concentration was created (Jia et al., 2009). Based on the explanations, the final voltage of a single fuel cell is as below:

$$V_T = E_N - V_c - V_\Omega - V_a \tag{2}$$

where, V_T describes the output voltage of the cell (V), E_N defines the open-circuit voltage (V), V_c defines the voltage reduction due to the reactant's gases concentration reduction or, due to the transport of mass of hydrogen and oxygen, V_Ω defines the ohmic voltage drop due to the protons conduction resistances over the solid electrolyte and the electrons by its path, V_a describes the voltage drop because of the activation of the cathode and anode.

In Eq. (4), E_N signifies the Nernst potential which is obtained by the following equation (Yu et al., 2019):

$$E_N = \frac{1}{2F} \times \left[\Delta G - \Delta S \times \left(T - T_{ref}\right) + R \times T \times \left(\ln P_{H_2} + \frac{\ln P_{O_2}}{2} \right) \right] \tag{3}$$

where T describes the performance temperature of the fuel in Kelvin, and P_{H_2}, and P_{H_2O} represent the partial pressures (atm) of Hydrogen and Oxygen, respectively, and are achieved by the following equation:

$$P_{H_2} = \frac{R_{ha} \times P_{H_2O}}{2} \times \left[\frac{P_a}{R_{ha} \times P_{H_2O} \times e^{\frac{1.635 I_{PEM}/A}{T^{1.334} I_{PEM}}}} - 1 \right] \tag{4}$$

$$P_{O_2} = R_{hc} \times P_{H_2O} \times \left[\frac{P_c}{R_{hc} \times P_{H_2O} \times e^{\frac{1.635 I_{PEM}/A}{T^{1.334} I_{PEM}}}} - 1 \right] \tag{5}$$

$$\begin{aligned} ln\left(P_{H_2O}\right) &= 2.95 \times 10^{-2} T_c - 9.18 \times 10^{-5} T_c^2 \\ &\quad + 1.4 \times 10^{-7} T_c^3 - 2.18 \end{aligned} \tag{6}$$

where, P_a and P_c describe the anode and cathode inlet pressure, and R_{ha} and R_{hc} signify the vapor's relative humidity at the anode and cathode, respectively.

Then, the analytical technique of the activation voltage drops (V_a) is given below:

$$V_{act} = \zeta_1 + \zeta_2 \times T + \zeta_3 \times T \times [ln\,(CO_2)] + \zeta_4 \times T \times [ln\,(I)] \tag{7}$$

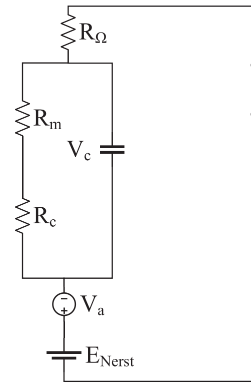

Fig. 2. The PEMFC with circuit model base.

where, I defines the PEMFC contemporary current value, ζ_i describes the amount of the *ith* pseudo empirical variable. The CO_2 entitles the concentration of Oxygen at cathode/gas interface that is achieved by the following:

$$CO_2 = p_{O_2} \times \left[5.08 \times 10^8 \times e^{\left(\frac{-498}{T}\right)} \right]^{-1} \tag{8}$$

Also, the ohmic voltage is achieved as follows:

$$V_\Omega = I \times R_\Omega = I \times (R_M + R_c) \tag{9}$$

where, R_c indicates the connection resistance, and R_m represents a resistance value achieved by the following equation:

$$R_m = \frac{r_M l}{S} \tag{10}$$

where, l denotes the membrane thickness, S stands for the membrane surface (cm^2), r_M defines the equivalent membrane impedance, and

$$r_M = \frac{181.6 \times \left[0.062 \left(\frac{T}{303}\right)^2 \times \left(\frac{I}{S}\right)^{2.5} + \left(\frac{3I}{100S}\right) + 1 \right]}{\left[\lambda - 0.063 - \left(\frac{3I}{S}\right)\right] \times e^{\frac{T-303}{T}}} \tag{11}$$

where, λ describes an adjustable variable.

And the concentration voltage drop is given below:

$$V_c = B \times \exp\left(Q \times \frac{i}{A}\right) \tag{12}$$

where, i describes the cell operating current (A), B and Q describe the diffusion's parameters (V and S^{-1}), S signifies the reactive area of the cell (cm^2).

Fig. 2 displays the circuit-based technique of the PEMFC with the explained mathematical modeling base.

3. Problem formulation

As seen in the previous section, the fuel cells model includes eight unknown parameters including ζ_1, ζ_2, ζ_3, ζ_4, R_c, λ, B, Q which should be obtained optimally. To achieve an optimal parameters selection, mean square error (MSE) has been considered. This function indicates the error between the actual observed produced terminal voltage and the estimated voltage based on the proposed technique. Indeed, the major concept here is to outline a new improved metaheuristic-based methodology for minimizing the MSE by proper choice of the unknown variables. The function MSE is given in the following:

$$MSE = \frac{1}{M} \sum_{j=1}^{M} \left(V_j - V_j^*\right)^2 \tag{13}$$

where, M stands for the number of experimental data; and V_j and V_j^* are the experimental data, and the simulated estimated data. The graphical abstract of the research is given in Fig. 3.

4. Methodology

4.1. Water Strider algorithm

Most of the optimization problems are so complicated, including interdependent variables, with nonlinear constraints, and a wide range of solutions (Ramezani et al., 2020; Tejani et al., 2017). For these difficult optimization problems for which there is no specific method for solving, metaheuristic optimization algorithms are a well-known and widely used method (Zhang et al., 2020a; Tejani et al., 2018a). The metaheuristics ensure that we can achieve a set of valuable variables to reach the goal of the objective function, considering the constraints of the function (Razmjooy et al., 2020). Many metaheuristic optimization techniques with several applications have been introduced in the last two decades, for example, mixed-integer genetic algorithm (Hamian et al., 2018), World Cup Optimizer (Navid Razmjooy and Ghadimi, 2018), antlion optimizer (Ramezani et al., 2020). The metaheuristics have been considered by researchers due to their simpleness, flexibility, no requirement for derivation and avoid from local optimality (Guo et al., 2020a). However, by No Free Lunch (NFL) Theory, it has been reasonably confirmed that no metaheuristic functions to find a solution for all optimization problems (Fan et al., 2020b). Namely, a specific metaheuristic can show promising achievements to solve a set of problems, but the selfsame algorithm can show weak operation for several other problems (Zhang et al., 2020b). Here, we propose a new enhanced technique that rely on Water Strider Algorithm (WSA) to solve the optimum choice of variables in the PEMFC technique. This algorithm imitates the territorial behavior of water strider insects, mating style, intelligent ripple coordination, feeding processes, and succession (Kaveh et al., 2020). The proposed algorithm provides an efficient performance to produce a good precision along with fast convergence.

4.2. Mathematical modeling

The Water Strider Algorithm includes five main phases: birth, creating territory, feeding, mating, death, and succession (Yanda et al., 2020).

(a) Birth

The water striders are born on the lake with eggs that are laid by females. For the sake of convenience, based on the algorithm, the initial population of the water striders is considered randomly and uniformly distributed. This case can be formulated as follows:

$$\begin{aligned} &X_i^0 = Lb + rand \times (Ub - Lb) \\ &i = 1, 2, \ldots, n. \end{aligned} \tag{14}$$

X_i^0 describes the initial location of the water strider number i, $rand$ describes a consistently random value between 0 and 1, n defines the number of water striders, Ub and Lb denotes the higher and lower boundaries of the problem, respectively.

Then, the water striders have been tested by the objective function in the problem after producing the initial water striders on the lake to determine the health of their location. In their role, the importance of the target feature depends on the availability of food.

(b) Establishing territory

The water striders live and exhibit territorial conduct in the territories. Partly a mature male (keystone) and some females (optimum foraging-habitat applicant) bugs are involved in each territory. The water striders are saved by their fitness in this algorithm to decide the n number of territories by overall n number of water striders. Then they are split into some groups, and each territory is assembled in a sorted way by taking one water striders from each group.

(c) Mating

Water striders occupy a large part of their lives to breeding or seeking to do so. The keystone of each territory in this phase generates definite courtship signals to a female via ripple signals. Afterward, the female gives feedback with either attraction to or keeping away from signals. So, the male starts mating if the females accept it, otherwise, due to her strong shield, the male cannot do the mating even if it violently mounts her. The mating of the Water striders is mathematically modeled below:

$$\begin{cases} X_i^{t+1} = X_i^t + R \times rand, & \text{if mating happens} \\ & (\text{with probability of } p) \\ X_i^{t+1} = X_i^t + R \times (1 + rand), & Otherwise \end{cases} \tag{15}$$

where, $rand$ stands for a random vector between 0 and 1, X_i^t represents the location for the water strider number i in the cycle number i.

Here, R signifies a vector that shows the distance between the location of male (X_i^t) and the endpoint is at the location of a female in that territory (X_F^t). The female here is obtained using a fitness comparable choice procedure like roulette wheel selection. Therefore, the term R is mathematically defined as follows:

$$R = X_F^t - X_i^t \tag{16}$$

(d) Foraging

The process of mating is an energy-intensive task, irrespective of its success. Therefore, water striders in the new location, feed to get enough energy.

Here, the objective role assesses the current location. If the previous condition is less than the objective value, this means that the food for regeneration has been uncovered. However, if the intrinsic importance is lower than the previous state, it should pass through the optimum territory that includes the highest fitness (X_{BL}^t). This process is formulated in the following equation:

$$X_i^{t+1} = X_i^t + 2 \times rand \times \left(X_{BL}^t - X_i^t\right) \tag{17}$$

(e) Death and succession

To guarantee the limitation of the search space among the water striders, after entering a strange water strider into the new territory, males demonstrate violent territorial behavior for Repelling the intruders. This repelling is too violent and maybe causes some murdering between intruders and residents. In this stage, if the previous position has a higher value than the objective value, the water strider will die and a new water strider will be substituted, otherwise, the keystone would continue alive. i.e.,

$$X_i^{t+1} = Lb_j^t + rand \times \left(Ub_j^t - Lb_j^t\right) \tag{18}$$

where, Ub_j^t and Lb_j^t represent the maximum and minimum values of the water strider's location inside territory number j.

(f) Termination condition

Finally, the algorithm will be ended if the termination condition has been reached. Otherwise, if the condition is not satisfied, the process of updating will be iterated based on new mating for new life cycles. Based on the Water Strider Algorithm conception, the maximum iteration has been selected as the termination condition.

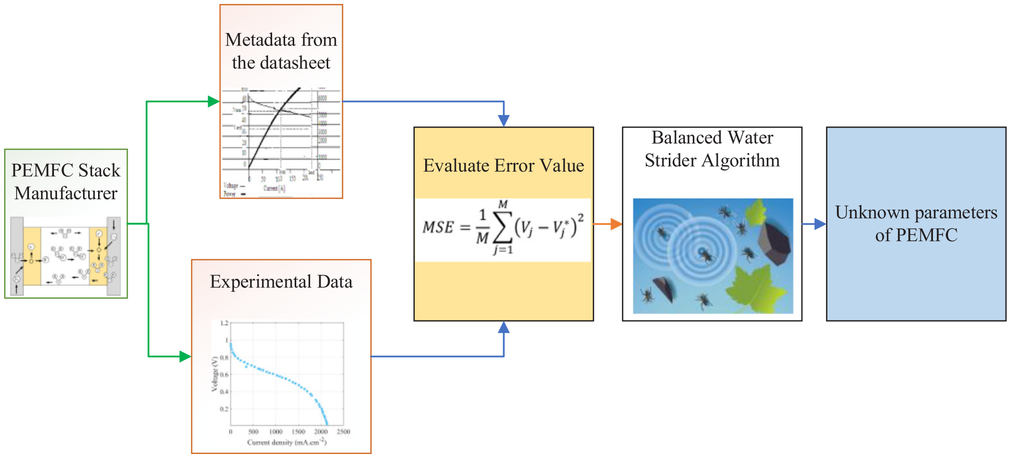

Fig. 3. The graphical abstract of the research.

4.3. *The balanced Water Strider Algorithm(bWSA)*

Any sorts of drawbacks affect the efficiency of the traditional Water Strider Algorithm, such as stability and premature convergence. This motivates us to outline an improved design of this algorithm to refine the weaknesses as much as possible. In this analysis, the Lévy flight (LF) acts as a chaotic mechanism used to boost the Slime Mold Algorithm's exploration and convergence ability. A random walking procedure for effective tuning of the local search was developed based on the Lévy flight, i.e. (Choi and Lee, 1998):

$$\mathrm{Le}\,(\mathrm{w}) \cong \frac{1}{\mathrm{w}^{\xi+1}} \tag{19}$$

$$\mathrm{w} = \frac{\mathrm{A}}{|\mathrm{B}|^{1/\xi}} \tag{20}$$

$$\sigma^2 = \left\{ \frac{\Gamma(1+\xi)}{\xi\,\Gamma((1+\xi)/2)}\, \frac{\sin(\pi\xi/2)}{2^{(1+\xi)/2}} \right\}^{\frac{2}{\xi}} \tag{21}$$

where, Γ (.) denotes the Gamma function, w defines the step size, A, B $\sim$ N$(0, \sigma^2)$, ξ determines the Lévy index in the range $(0, 2]$. Based on (Li et al., 2018), in this study, the value of the ξ is set 3/2.

By the Lévy flight, the new location of the foraging and Death and succession can be updated as follows:

$$X_i^{t+1} = X_i^t + 2 \times \mathrm{Le}(\delta) \times \left(X_{BL}^t - X_i^t\right) \tag{22}$$

$$X_i^{t+1} = Lb_j^t + rand \times \left(Ub_j^t - Lb_j^t\right) \tag{23}$$

where, X_i^{t+1} indicates the new location for the $(i+1)^{th}$ candidate and,

$$A = a \times (2 \times r - 1) \tag{24}$$

$$B = C \times f(t) - X(t) \tag{25}$$

where, r signifies a random magnitude in the range [0, 1], a determines a parameter between 0 and 2, and $f(t)$ defines random location vector.

Fig. 4 shows the flowchart diagram of the proposed bWSA.

4.4. *Experimental validation of the algorithm*

The proposed balanced Water Strider Algorithm (bWSA) which is mentioned in the former section is programmed by the MATLAB 2017b and all of the tests are applied to a CoreTM i7-4720HQ 1.60 GHz with 16 GB RAM Laptop machine. The bWSA has been validated by implementing it into some standard benchmark functions, i.e. Six-hump-camel, Levi No. 03 function, Schweffel function, and Leon function and a comparison of the results with several various metaheuristics including Locust Swarm Optimization (LSO) (Cuevas et al., 2020), Multi-verse optimize (MVO) (Mirjalili et al., 2016), Spotted hyena optimize (SHO) (Dhiman and Kumar, 2017), and the original Water Strider Algorithm (WSA) (Kaveh et al., 2020) is carried out. The explanations of the employed test problems are given below.

The first test function is Six-hump-camel. The profile of this function is shown in (Fig. 3-f_1). As can be observed, the function contains six local minimum points, where two of them are global. The limitation of the variables is: $x_1 = [-3, 3]$ and $x_2 = [-2, 2]$. The formulation of this function is given in the following equation :

$$\mathrm{F}_1\,(\mathrm{x}) = \left(4 - 2.1x_1^2 + \frac{x_1^4}{3}\right)x_1^2 + x_1x_2 + \left(-4 + 4x_2^2\right)x_2^2 \tag{26a}$$

The second test function is Levi No. 03 function. This function is continuous and non-convex. The Levi No. 03 function has a 2-dimensional search space that defines a multimodal problem (Tejani et al., 2016, 2019, 2018b). The limitation for all variables is between -10 and 10. Subsequently, the fitness function of the Levi No. 03 is shown below:

$$F_2\,(x) = \sin^2(3\pi x_1) + (x_1 - 1)^2\left(1 + \sin^2(3\pi x_2)\right) + (x_2 - 1)^2\left(1 + \sin^2(2\pi x_2)\right) \tag{26b}$$

The third function is Schweffel function. This function is so complicated with numerous local minima. A two-dimensional form of this function is shown in (Fig. 3-f_3). The feasible interval for this function is regularly considered on an n-dimension hypercube between -500 and 500, i.e.

$$\mathrm{F}_3\,(\mathrm{x}) = 418.9829d - \sum_{i=1}^{d} x_i \sin\left(\sqrt{|x_i|}\right) \tag{26c}$$

The last function is Leon. The Leon function is a continuous and non-convex function with a 2-dimensional search space. The function is also differentiable and unimodal. The Leon function is a non-separable function in the range [0, 10]. The formula for this function is given below:

$$\mathrm{F}_4\,(\mathrm{x}) = 100\left(\mathrm{x}_2 - \mathrm{x}_1^3\right)^2 + (1 - x_1)^2 \tag{26d}$$

Fig. 5 displays a 2d profile of the tested functions.

As before mentioned, for validating the operation of the suggested technique, it is compared with various algorithms to simplify the analysis for the readers, the used parameter specific for each algorithm are given in Table 1.

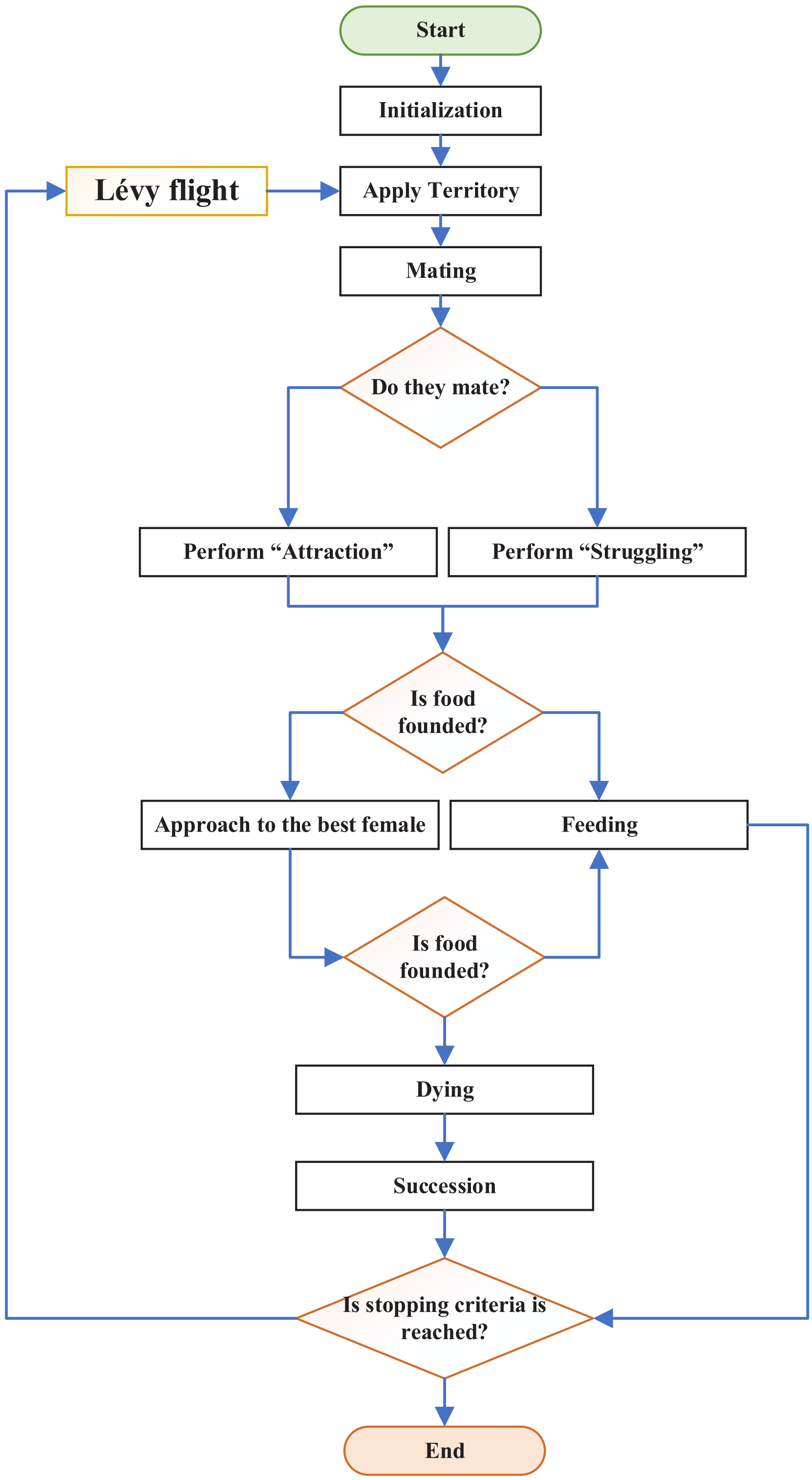

Fig. 4. The flowchart diagram of the proposed bWSA.

Table 1
The used variable specific for each algorithm.

Algorithm	Parameter	Value	Algorithm	Parameter	Value
LSO (Cuevas et al., 2020)	F	0.6	ALO (Mani et al., 2018)	w	[2, 6]
	L	1		No. search agents	50
	g	20	MVO (Mirjalili et al., 2016)	Traveling distance rate	[0.6, 1]
SHO (Dhiman and Kumar, 2017)	$\vec{M}$	[0.5, 1]		Wormhole existence probability	[0.2, 1]
	$\vec{h}$	[5, 0]			

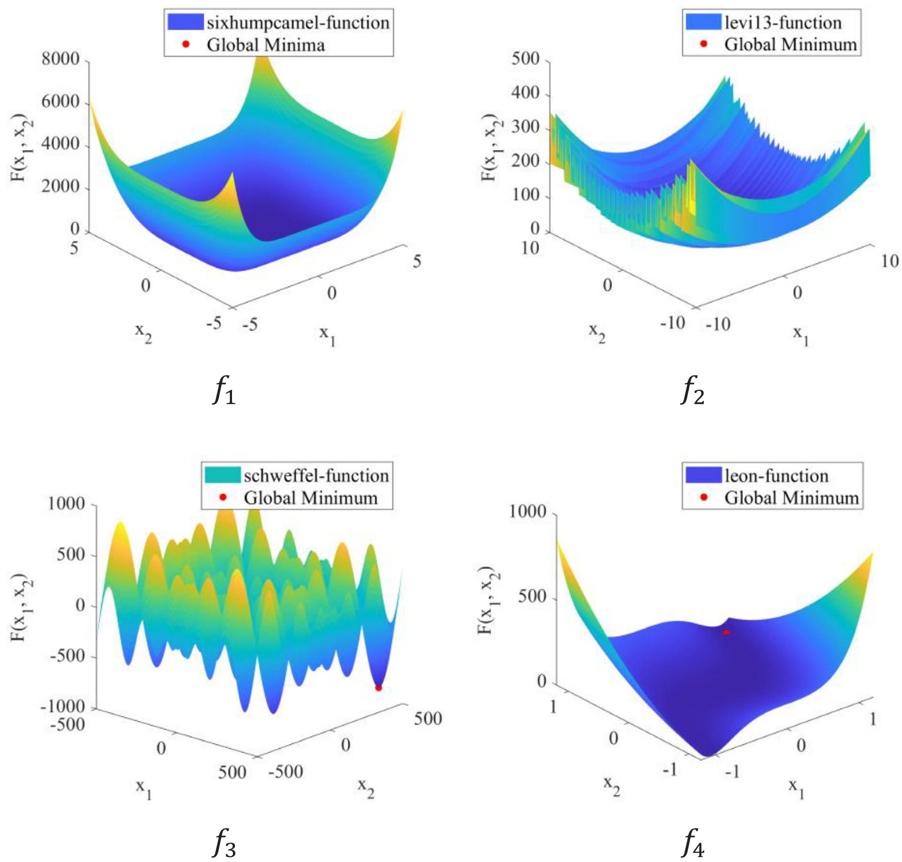

Fig. 5. 2d profile of the tested functions.

Table 2
The comparison analysis of the algorithms applied to the test functions.

Algorithm		f_1	f_2	f_3	f_4
LSO (Cuevas et al., 2020)	Min	8.6429e−8	7.5021	4.2719	3.4855e−7
	Max	16.4815e−3	21.5423	12.4561	25.6325e−4
	Mean	24.6147e−5	11.8569	8.7459	11.4533e−5
	std	11.3248e−6	18.8456	7.2578	8.3762e−7
SHO (Dhiman and Kumar, 2017)	Min	16.4315e−13	2.5038	1.4533e−3	2.1663e−4
	Max	34.1542e−9	3.4718	3.5849e−1	3.2934e−3
	Mean	19.4428e−10	3.7934	2.3570e−2	18.7718e−3
	std	21.6152e−11	3.4708	1.3481e−2	3.1562e−4
MVO (Mirjalili et al., 2016)	Min	19.5126e−18	1.4712	2.6745e−5	1.4512e−3
	Max	28.4612e−14	2.8793	0.2516	74.156e−2
	Mean	31.6728e−16	1.9985	0.1549	12.8628e−2
	std	16.4832e−17	1.5249	3.6039e−3	8.3721e−3
WSA (Kaveh et al., 2020)	Min	25.2941e−22	0.3854	3.5478e−8	27.2743e−8
	Max	8.8745e−19	1.9057	10.8996e−6	19.8946e−6
	Mean	16.4692e−20	1.8314	2.3876−7	48.7845e−7
	std	11.2461e−21	0.3969	3.9833e−8	30.6215e−8
bWSA	Min	32.8164e−27	21.7053e−6	5.8877e−11	1.7831e−15
	Max	2.5235e−23	1.4124e−2	3.3857e−10	7.1687e−8
	Mean	46.9452e−24	35.8341e−3	1.4589−10	3.4286e−10
	std	22.8348e−25	11.7234e−4	5.2378e−11	1.4562e12

In all of the simulations in the algorithms, the individual size for the agents is set at 100. Also, the simulations have been performed 30 times independently to give a consistent result. Finally, the numbers of iteration for the algorithms are considered 200. The comparison analysis based on four indicators including minimum (min), maximum (max), mean value (mean), and standard deviation (Std) value for all of the algorithms applied to the test functions is stated in Table 2.

As seen in Table 2, the suggested bWSA technique with a minimum value of min, max, and mean values rather than the others indicates higher precision of the method against the other compared methods. Similarly, based on the achievements, the standard deviation amount in the algorithm is the lowest amount among the other latest techniques. This shows the higher reliability of the suggested bWSA toward the other compared algorithms. Moreover, the algorithms' convergence analysis applied to the test functions is also depicted in Fig. 6.

As seen in Fig. 6, the proposed bWSA in all analyzed cost functions has the fastest convergence which is parallel with a correct convergence, not a premature one. So, we can conclude

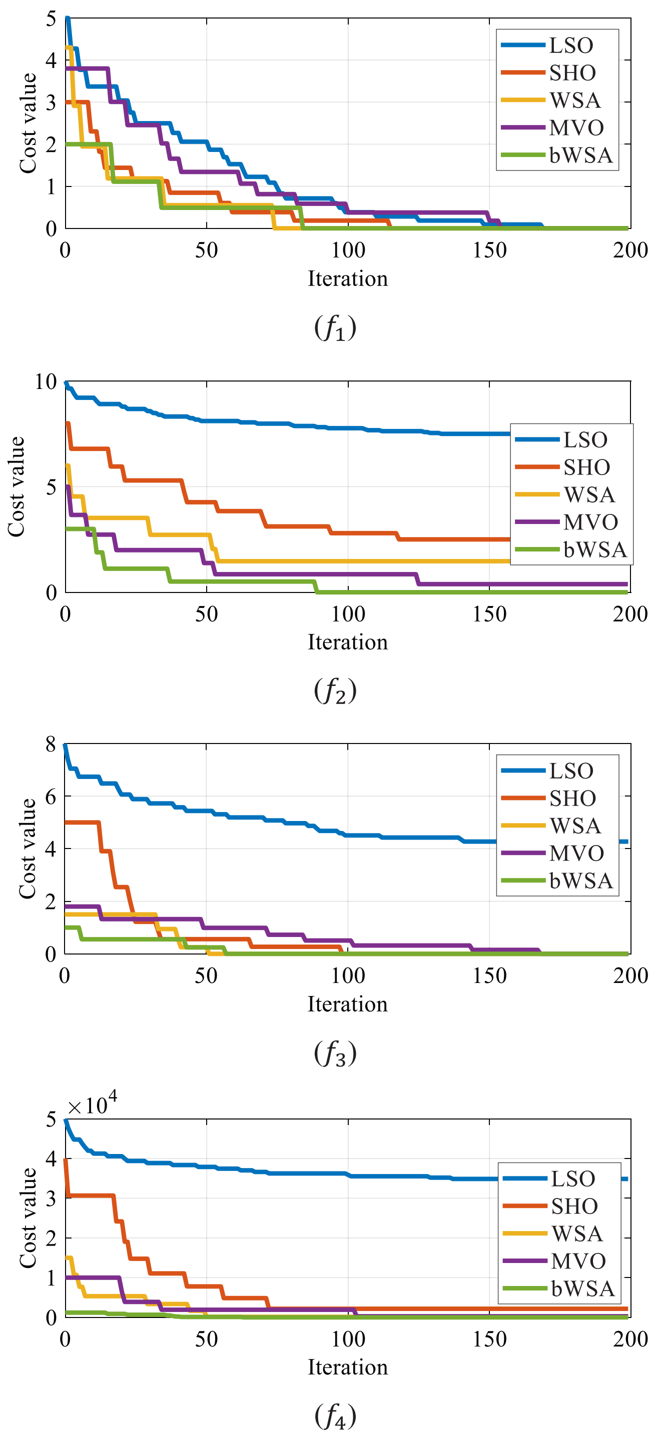

Fig. 6. The algorithms' convergence assessment applied to the test functions.

that the suggested algorithm gives a good accuracy to use as a PEMFC model parameter estimation in this study.

5. Simulation results

For analysis the proposed methodology, it has been performed on the PEMFC test system from the Fuel Cell Application Centre (FAC) of the Temasek Polytechnic Engineering School (Jia et al., 2009).

Table 3
The required specifications of the 20-cell stack test case.

Parameter	Value
Electrolyte membrane	Nafion 112
Pt loading	0.4 mg/cm^2
Active area	150 cm^2
T_{PEMFC}	323 K
P	0.5 atm
Resolution of cooling system	0.1 °C

5.1. The 20-cel stack

In this case, we utilized a 20-cell stack outlined and created by Singapore GasHub and FAC. The simulation achievement of the suggested bWSA are then compared with various algorithms from the literature including Wildebeest Herd Optimization (WHO) (Amali and Dinakaran, 2019), Search and rescue optimization algorithm (SAR) (Shabani et al., 2020), World Cup Optimizer (WCO) (Razmjooy et al., 2016), Elephant Herding Optimizer (EHO) (Wang et al., 2015), Firefly algorithm (FA) (Yang, 2008), and the original Water Strider Algorithm (WSA) (Kaveh et al., 2020). Table 3 tabulates the required specifications of this test case.

5.2. The results

To analyze the steady-state response of the PEMFC stack before entering it, both the air and the hydrogen have been humidified. To give a self-humidification of the hydrogen at the anode side, the hydrogen recycling pump has been employed. Also, the humidification for the air is 100% that is done by EFH-100WA solid-state humidifier from EnerFuel, Inc. (Ener Fuel Inc, 2020). Polarization measurements have been performed to obtain stable efficiency before a steady state. Based on (Jia et al., 2009), the voltage–current polarization and the voltage response for the cell/stack have been measured by LeCroy Waverunner LT344 and Scribner Associates 890CL. In order to govern the airflow and Hydrogen flow thereby recording the answer of the produced voltage and to reduce the latency of the gas pipe, the mass flow controls with the electromagnetic amounts are installed; the humidifiers have been employed to avoid dehydration of the fuel cell membrane and boost the reaction rate; a hydrogen purge device by segregators is performed to the fuel utility increasing. The cooling system is based on Julabo FP40 model that is controlled by a PID controller for temperature regulation. The general diagram of the case study is shown in Fig. 7.

To give a proper validation for the proposed method, as before mentioned, its optimization results have been compared with WHO (Amali and Dinakaran, 2019), SAR (Shabani et al., 2020), WCO (Razmjooy et al., 2016), EHO (Wang et al., 2015), FA (Yang, 2008), and the original WSA (Kaveh et al., 2020). Simulations have been performed by MATLAB 2017b Simulink and the programs have been coded by MATLAB Script. The individual size for the agents is set 100. Also, the simulations have been performed 30 times independently to give a consistent result, and the number of iteration for the algorithms are considered 200. Table 4 illustrates used parameters specific to each algorithm.

For giving a proper comparison between the proposed method and the other methods, four measurement indicators including optimum (Best), worst (Worst), the average amount (Mean) and the standard deviation (Std) of the cost function that is explained before have been performed. The results of the parameters achieved by the algorithms and the comparison achievements are stated in Tables 5 and 6, respectively.

As seen in Table 6, the suggested bWSA provides the lowest amount for Best, Worst, and Mean values. This means that the

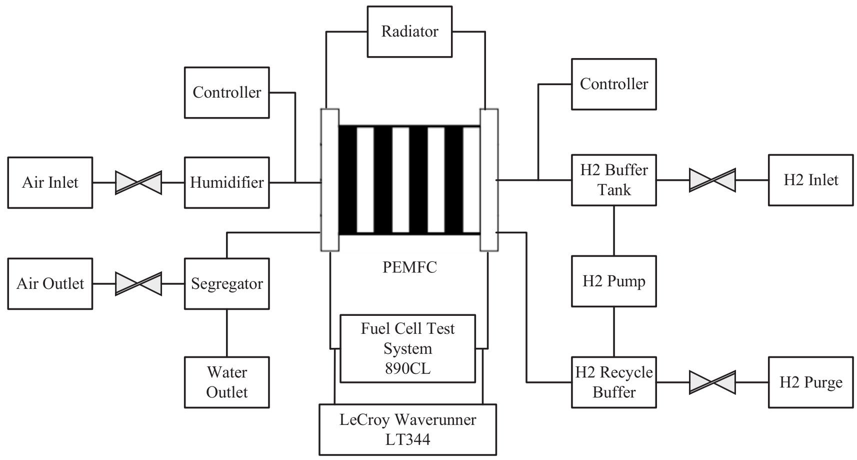

Fig. 7. The general diagram of the case study.

Table 4
The used parameter specific for each algorithm.

Algorithm	Parameter	Value	Algorithm	Parameter	Value
WHO (Amali and Dinakaran, 2019)	α_1	0.9	EHO (Wang et al., 2015)	R	1000
	β_1	0.3		nClan	4
	α_2	0.2		α	0.25
	β_2	0.8		β	0.05
SAR (Shabani et al., 2020)	*SE*	0.5		γ	0.02
	MU	20	FA (Yang, 2008)	α	0.2
WCO (Razmjooy et al., 2016)	Play off	0.04		β	0.5
	ac	0.3		γ	1

Table 5
The achievements of the parameters achieved by the algorithms.

	WHO (Amali and Dinakaran, 2019)	SAR (Shabani et al., 2020)	WCO (Razmjooy et al., 2016)	EHO (Wang et al., 2015)	FA (Yang, 2008)	WSA (Kaveh et al., 2020)	bWSA
ξ_1	−8.8189e−1	−8.5130e−1	−8.7546e−1	−8.7935e−1	−8.5184e−1	−8.5615e−1	−8.6535e−1
ξ_2	3.4930e−3	3.8805e−3	3.3688e−3	4.0836e−3	4.1621e−3	3.9527e−3	3.3361
ξ_3	7.3889e−5	1.0063e−4	7.3836e−5	1.1982e−4	1.1775e−4	1.0389e−4	7.3889e−5
ξ_4	−1.4889e−4	−1.4001e−4	−1.4889e−4	−1.4889e−4	−1.4889e−4	−1.4917e−4	−1.4889e−4
R_c	6.3859e−3	5.9795e−3	5.3645e−3	6.3847e−3	6.3593e−3	5.9601e−3	6.3857e−3
λ	2.2889e+1	1.5829e+1	1.0000e+1	2.2889e+1	1.0000e+1	1.7271e+1	2.2889e+1
B	1.6389e−4	3.9148e−4	6.4848e−4	1.6089e−4	1.6389e−4	2.3350e−4	1.6389e−4
Q	3.5953e−3	3.1134e−3	2.9107e−3	3.5853e−3	3.5823e−3	3.3531e−3	3.5852e−3

Table 6
The comparison result of the studied algorithms.

	WHO (Amali and Dinakaran, 2019)	SAR (Shabani et al., 2020)	WCO (Razmjooy et al., 2016)	EHO (Wang et al., 2015)	FA (Yang, 2008)	WSA (Kaveh et al., 2020)	bWSA
Best	3.4831e−4	3.8167e−4	3.9114e−4	3.4831e−4	3.5805e−4	3.6554e−4	3.4831e−4
Worst	7.2938e−2	1.3842e−3	2.8963e−3	3.6387e−4	3.8890e−4	4.1187e−4	3.5401e−4
Mean	3.5240e−3	6.4714e−4	0.9208e−3	3.5352e−4	3.6587e−4	3.7812e−4	3.4857e−4
Std	1.2117e−2	2.2057e−4	5.4238e−4	4.4108e−6	0.9426e−5	9.8135e−6	0.9130e−6

proposed method after 30 self-reliant runs has the minimum amount for the SSE of the parameter fitting in the PEMFC and has the best accuracy among them. Also, by a glance at Table 6, it can be observed that the standard deviation value in the proposed bWSA gives the smallest value that shows its proper reliability in comparison to other algorithms. The dominance of the suggested algorithm is also observable in Fig. 8.

As can be shown in Fig. 8, the proposed bWSA has the fastest run time toward the other latest algorithms. Finally, the fitting curve of five better algorithms has been shown in Fig. 9.

As seen in Fig. 9, after applying 30 runs and plotting a mean value of the algorithms, the proposed method with minimum absolute error equals 3.4831e−4 gave the best results in comparison to the other techniques. Therefore, simulations displayed a suitable agreement between the estimated and the real values of the PEMFC model for almost all of the algorithms, especially for the proposed bWSA.

6. Conclusions

Fuel cells are new kinds of energy generation technologies that convert chemical energy directly to electricity. One of the well-known kinds of these energy production systems is Proton-exchange membrane fuel cells (PEMFCs) that have several advantages over the others. A disadvantage of these energy conversion systems is their construction cost. The major target of this paper was to optimize the model parameters of a PEMFC to minimize this cost as much as possible. The idea was to lessen the Sum

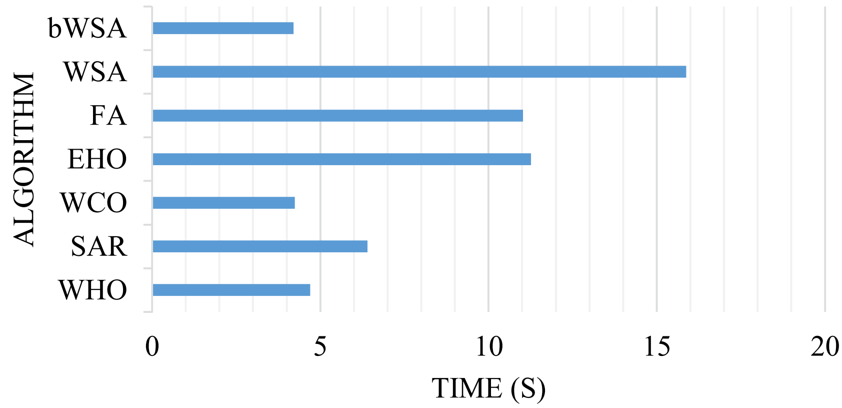

Fig. 8. Elapsed time for the studied algorithms for PEMFC parameters identification.

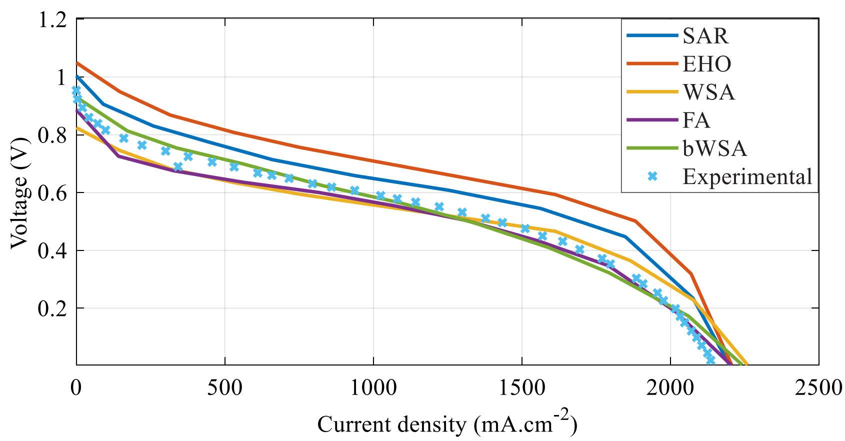

Fig. 9. The fitting curve of five better algorithms.

of Squared Error (SSE) amount between the empirical produced voltage and the approximated produced voltage. To give better results in terms of accuracy and reliability, a new design of a new metaheuristic called balanced Water Strider Algorithm (bWSA) was employed. The results of the suggested method were first validated by comparing with several algorithms and then used for verification by applying it to a practical test case (a 20-cell stack). Also, a comparison of the results of simulation with several various latest techniques was carried out. The results were performed to a practical test case. After running all of the optimizers 30 times independently, the proposed method with minimum absolute error equals 3.4831e−4 provided the best results against the compared methods.

CRediT authorship contribution statement

Rahmad Syah: Conceptualization, Data curation, Writing – original draft, Writing – review & editing. **Lawal Adedoyin Isola:** Conceptualization, Data curation, Writing – original draft, Writing – review & editing. **John William Grimaldo Guerrero:** Conceptualization, Data curation, Writing – original draft, Writing – review & editing. **Wanich Suksatan:** Conceptualization, Data curation, Writing – original draft, Writing – review & editing. **Denok Sunarsi:** Conceptualization, Data curation, Writing – original draft, Writing – review & editing. **Marischa Elveny:** Conceptualization, Data curation, Writing – original draft, Writing – review & editing. **Ayad F. Alkaim:** Conceptualization, Data curation, Writing – original draft, Writing – review & editing. **Lakshmi Thangavelu:** Conceptualization, Data curation, Writing – original draft, Writing – review & editing. **Surendar Aravindhan:** Conceptualization, Data curation, Writing – original draft, Writing – review & editing.

Declaration of competing interest

The authors declare that they have no known competing financial interests or personal relationships that could have appeared to influence the work reported in this paper.

References

Aghajani, G., Ghadimi, N., 2018. Multi-objective energy management in a micro-grid. Energy Rep. 4, 218–225.
Amali, D., Dinakaran, M., 2019. Wildebeest herd optimization: A new global optimization algorithm inspired by wildebeest herding behaviour. J. Intell. Fuzzy Systems (Preprint), 1–14.
Bagheri, M., et al., 2018. A novel wind power forecasting based feature selection and hybrid forecast engine bundled with honey bee mating optimization. In: 2018 IEEE International Conference on Environment and Electrical Engineering and 2018 IEEE Industrial and Commercial Power Systems Europe (EEEIC/I & CPS Europe. IEEE.
Cai, W., et al., 2019. Optimal bidding and offering strategies of compressed air energy storage: A hybrid robust-stochastic approach. Renew. Energy 143, 1–8.
Choi, C., Lee, J.-J., 1998. Chaotic local search algorithm. Artif. Life Robot. 2 (1), 41–47.
Cuevas, E., Fausto, F., González, A., 2020. The locust swarm optimization algorithm. In: New Advancements in Swarm Algorithms: Operators and Applications. Springer, pp. 139–159.
Dhiman, G., Kumar, V., 2017. Spotted hyena optimizer: a novel bio-inspired based metaheuristic technique for engineering applications. Adv. Eng. Softw. 114, 48–70.
2020. Ener fuel inc. Available from: https://www.enerfuel.com/humid2.aspx.

Fan, X., et al., 2020a. High voltage gain DC/DC converter using coupled inductor and VM techniques. IEEE Access 8, 131975-131987.
Fan, X., et al., 2020b. Multi-objective optimization for the proper selection of the best heat pump technology in a fuel cell-heat pump micro-CHP system. Energy Rep. 6, 325–335.
Fei, X., Xuejun, R., Razmjooy, N., 2019. Optimal configuration and energy management for combined solar chimney, solid oxide electrolysis, and fuel cell: a case study in Iran. Energy Sources A 1–21.
Ghiasi, M., Ghadimi, N., Ahmadinia, E., 2019. An analytical methodology for reliability assessment and failure analysis in distributed power system. SN Appl. Sci. 1 (1), 44.
Guo, Y., et al., 2020a. An optimal configuration for a battery and PEM fuel cell-based hybrid energy system using developed Krill herd optimization algorithm for locomotive application. Energy Rep. 6, 885–894.
Guo, H., et al., 2020b. Optimized parameter estimation of a PEMFC model based on improved grass Fibrous root optimization algorithm. Energy Rep. 6, 1510–1519.
Hamian, M., et al., 2018. A framework to expedite joint energy-reserve payment cost minimization using a custom-designed method based on mixed integer genetic algorithm. Eng. Appl. Artif. Intell. 72, 203–212.
Hosseini Firouz, M., Ghadimi, N., 2016. Optimal preventive maintenance policy for electric power distribution systems based on the fuzzy AHP methods. Complexity 21 (6), 70–88.
Jia, J., et al., 2009. Modeling and dynamic characteristic simulation of a proton exchange membrane fuel cell. IEEE Trans. Energy Convers. 24 (1), 283–291.
Kaveh, A., Eslamlou, A.D., Khodadadi, N., 2020. Dynamic water strider algorithm for optimal design of skeletal structures. Period. Polytech. Civ. Eng. 64 (3), 904–916.
Li, X., Niu, P., Liu, J., 2018. Combustion optimization of a boiler based on the chaos and levy flight vortex search algorithm. Appl. Math. Model. 58, 3–18.
Liu, J., et al., 2020. An IGDT-based risk-involved optimal bidding strategy for hydrogen storage-based intelligent parking lot of electric vehicles. J. Energy Storage 27, 101057.
Mani, M., Bozorg-Haddad, O., Chu, X., 2018. Ant lion optimizer (ALO) algorithm. In: Advanced Optimization By Nature-Inspired Algorithms. Springer, pp. 105–116.
Meng, Q., et al., 2020. A single-phase transformer-less grid-tied inverter based on switched capacitor for PV application. J. Control Autom. Electr. Syst. 31 (1), 257–270.
Mir, M., et al., 2020. Application of hybrid forecast engine based intelligent algorithm and feature selection for wind signal prediction. Evol. Syst. 11 (4), 559–573.
Mirjalili, S., Mirjalili, S.M., Hatamlou, A., 2016. Multi-verse optimizer: a nature-inspired algorithm for global optimization. Neural Comput. Appl. 27 (2), 495–513.
Navid Razmjooy, F.R.S., Ghadimi, Noradin, 2018. A hybrid neural network – world cup optimization algorithm for melanoma detection. Open Med. 13, 9–16.
Ramezani, M., Bahmanyar, D., Razmjooy, N., 2020. A new optimal energy management strategy based on improved multi-objective antlion optimization algorithm: applications in smart home. SN Appl. Sci. 2 (12), 1–17.
Razmjooy, N., Estrela, V.V., Loschi, H.J., 2020. Entropy-based breast cancer detection in digital mammograms using world cup optimization algorithm. Int. J. Swarm Intell. Res. (IJSIR) 11 (3), 1–18.
Razmjooy, N., Khalilpour, M., Ramezani, M., 2016. A new meta-heuristic optimization algorithm inspired by FIFA world cup competitions: theory and its application in PID designing for AVR system. J. Control Autom. Electr. Syst. 27 (4), 419–440.
Razmjooy, N., Ramezani, M., Ghadimi, N., 2017. Imperialist competitive algorithm-based optimization of neuro-fuzzy system parameters for automatic red-eye removal. Int. J. Fuzzy Syst. 19 (4), 1144–1156.
Saeedi, M., et al., 2019. Robust optimization based optimal chiller loading under cooling demand uncertainty. Appl. Therm. Eng. 148, 1081–1091.
Shabani, A., et al., 2020. Search and rescue optimization algorithm: A new optimization method for solving constrained engineering optimization problems. Expert Syst. Appl. 161, 113698.
Tejani, G.G., Savsani, V.J., Patel, V.K., 2016. Adaptive symbiotic organisms search (SOS) algorithm for structural design optimization. J. Comput. Des. Eng. 3 (3), 226–249.
Tejani, G.G., et al., 2017. Topology, shape, and size optimization of truss structures using modified teaching-learning based optimization. Adv. Comput. Des. 2 (4), 313–331.
Tejani, G.G., et al., 2018a. Size, shape, and topology optimization of planar and space trusses using mutation-based improved metaheuristics. J. Comput. Des. Eng. 5 (2), 198–214.
Tejani, G.G., et al., 2018b. Truss optimization with natural frequency bounds using improved symbiotic organisms search. Knowl.-Based Syst. 143, 162–178.
Tejani, G.G., et al., 2019. Topology optimization of truss subjected to static and dynamic constraints by integrating simulated annealing into passing vehicle search algorithms. Eng. Comput. 35 (2), 499–517.
Tian, M.-W., et al., 2020. New optimal design for a hybrid solar chimney, solid oxide electrolysis and fuel cell based on improved deer hunting optimization algorithm. J. Cleaner Prod. 249, 119414.
Wang, G.-G., Deb, S., Coelho, L.d.S., 2015. Elephant herding optimization. In: 2015 3rd International Symposium on Computational and Business Intelligence (ISCBI). IEEE.
Xu, H., et al., 2020. Exergy analysis and optimization of a HT-PEMFC using developed manta ray foraging optimization algorithm. Int. J. Hydrogen Energy 45 (55), 30932–30941.
Yanda, L., Yuwei, Z., Razmjooy, N., 2020. Optimal arrangement of a micro-CHP system in the presence of fuel cell-heat pump based on metaheuristics. Int. J. Ambient Energy 1–12.
Yang, X.-S., 2008. Firefly algorithm.
Yang, Z., et al., 2020. Model parameter estimation of the PEMFCs using improved barnacles mating optimization algorithm. Energy 118738.
Ye, H., et al., 2020. High step-up interleaved dc/dc converter with high efficiency. Energy Sources A 1–20.
Yin, Z., Razmjooy, N., 2020. PEMFC identification Using deep learning developed by improved deer hunting optimization algorithm. Int. J. Power Energy Syst. 40 (2).
Yu, D., Ghadimi, N., 2019. Reliability constraint stochastic UC by considering the correlation of random variables with copula theory. IET Renew. Power Gener. 13 (14), 2587–2593.
Yu, D., et al., 2019. System identification of PEM fuel cells using an improved elman neural network and a new hybrid optimization algorithm. Energy Rep. 5, 1365–1374.
Yu, D., et al., 2020. Energy management of wind-PV-storage-grid based large electricity consumer using robust optimization technique. J. Energy Storage 27, 101054.
Yuan, Z., et al., 2020. A new technique for optimal estimation of the circuit-based PEMFCs using developed sunflower optimization algorithm. Energy Rep. 6, 662–671.
Zhang, G., Xiao, C., Razmjooy, N., 2020a. Optimal operational strategy of hybrid PV/Wind renewable energy system using homer: A case study. Int. J. Ambient Energy 1–33.
Zhang, G., Xiao, C., Razmjooy, N., 2020b. Optimal parameter extraction of PEM fuel cells by meta-heuristics. Int. J. Ambient Energy 1–10.